Caractérisation du comportement en fluage à haute température de composites C/PEKK à matrice thermoplastique pour applications aéronautiques

Giuseppe Pedoto, Marco Gigliotti, Jean-Claude Grandidier

Caractérisation du comportement à fluage des composites à matrice thermoplastique pour applications aéronautiques à haute températures

Characterization of the creep behavior of thermoplastic matrix composites for aircraft applications at high temperatures

Giuseppe Pedoto[1], Marco Gigliotti[1] et Jean-Claude Grandidier[1]

1 : Département Physique et Mécanique des Matériaux, Institut Pprime
CNRS, ISAE-ENSMA, Université de Poitiers
1, avenue Clément Ader, F-86962 Futuroscope Chasseneuil, France
e-mail : giuseppe.pedoto@ensma.fr, marco.gigliotti@ensma.fr, jean-claude.grandidier@ensma.fr

Résumé

Cette étude est centrée sur la caractérisation des propriétés thermomécaniques du PEKK semi-cristallin et des composites à matrice thermoplastique C/PEKK : en particulier, sur la caractérisation, la modélisation et la simulation de leur comportement au fluage à des températures supérieures à la température de transition vitreuse. La phase de caractérisation consiste en une campagne d'essais DSC, DMA et de traction suivie d'une campagne expérimentale de fluage sur le polymère pur et les composites ±45°. Une modèle de micromécanique simple confirme qu'au premier ordre les comportements mécanique et physique de la matrice et la résine sont très proches.

Abstract

This study is focused on the characterization of the thermomechanical properties of semicrystalline PEKK and of C/PEKK thermoplastic based laminated composites: in particular, it is focused on the characterization, modeling and simulation of their creep behavior at temperatures above the glass transition temperature. The characterization phase consists in a preliminary campaign of DSC, DMA and tensile tests followed by an experimental creep test campaign on both the pure polymer and ±45° composites. A simple micromechanical model confirms that at the first order the mechanical and physical behavior of the matrix and the resin are very similar.

Mots Clés : composites, matrices thermoplastiques, fluage, température au-dessus de Tg
Keywords : composites, thermoplastics matrix, creep, temperature above Tg

1. Introduction

In the past 60 years, the aeronautic industry has progressively replaced a larger percentage of metal components with carbon fiber reinforced polymers, aiming for mass and cost reduction of aircraft structures. Furthermore, in the last 30 years, different studies have been carried out to replace the thermoset polymers employed as composites' matrices with thermoplastic polymers, to increase the maximum operational temperatures and because of the possibility to be recycled.

This study is part of the project ANR IMPEKKABLE, which aims to employ PolyEtherKetoneKetone (PEKK) as carbon fiber reinforced matrix to replace metallic components in the aircraft pylons. Such structures have operative conditions limit of 180°C (higher than PEKK's Tg) at 70% of their maximum load for a duration of at least 10 min (creep condition). The aim of the project is therefore to define the Material Operating Limit and to simulate the operating conditions.

The PEKK is a semicrystalline polymer of the PAEK family, with properties similar to the more diffused PEEK. It has been shown that the presence of the crystalline phase for PEEK ([1]) reduces the properties loss registered in almost amorphous PEEK if the temperature is raised above Tg. Other studies, carried out on the PEEK below its Tg, have shown the presence of physical ageing and the possibility of correcting the WLF law to obtain a time-temperature superposition ([2], [3]).

Different studies on the PEKK have shown the impact of the crystalline phase percentage, produced during the manufacturing process, on its mechanical properties below and above Tg=160°C ([4]). The presence of chemical phenomena at temperatures higher than Tg has been shown, and in particular between 250°C and Tm=330°C, where the material degrades because of oxidation and morphological changes appear, ([5]). Consequently, 250°C is a limit for using these composites, but how does the material behave between Tg and temperature limit?

This study aims at characterizing the semicrystalline PEKK behavior in the range of temperature between 160°C and 200°C, where not only physical ageing should not be possible, but also oxidation phenomena should be negligible for the temperature exposition taken into account. Those considerations lead to suppose, for the PEKK, a rheologically simple behavior in this range of temperature (describable by a WLF law). Furthermore, in this range of temperature, the presence of the crystalline phase in PEKK should reduce the properties loss due to the amorphous phase, if the temperature is raised above Tg, as seen for the PEEK.

It has been shown ([4],[6]) that the presence of the fibers changes the crystallization kinetics, in addition to the constraints applied to the matrix by the fiber themselves, leading to question if the behavior of the matrix inside the composite is similar to the pure resin's one and setting a second objective.

2. Materials and measurement system

2.1 Materials

The materials tested in this study are: the semicrystalline PEKK 7002, obtained from Arkema, and the $[(\pm 45°)_2, +45°]_s$ composite, obtained from Airbus and manufactured from prepregs of semicrystalline PEKK 7002 and AS4C carbon fibers. The properties of semicrystalline PEKK are listed in Tab.1.

Property	Value
Glass transition temperature - Tg	160°C
Melting temperature - Tm	330°C
Crystalline phase % - χ	24% (max)

Tab. 1. PEKK 7002 properties

2.2 Measurement system

The Videotraction System, a measurement system developed at the ISAE-ENSMA, was employed during all the tensile and creep tests under high temperature. It employs a video camera, which records the gauge length of the specimen were 4 markers are painted. Through the IdPix software, the system evaluates their centers of mass and, exploiting finite difference method, it is capable to measure the true strains and true stresses in real time. Furthermore, it requires a low definition camera only, implying low data volume. However, the test temperatures and the large measured deformations produce a degradation of the marker's paint.

A possible verification of the measurements could have been done through the employment of Digital Image Correlation (DIC). This technique requires a pattern instead of markers and high definition images, forcing the repetition of the whole test campaign. Moreover it employs a searching windows that need a predictive formulation to estimate the subsequent position of the searching window itself ([7]) and it results with the fact that it could not be able to follow the whole test duration, precisely because of the large measured deformations.

For those reasons, the DIC was excluded and a post-test measurement system was developed, the Image Analysis Tool (IAT), capable or reconstructing the degraded markers and fitting their

perimeter with an ellipse. This allows to obtain 5 points (major and minor axis ends and their intercept) for each markers, instead of just one. The coordinates of those 20 points are then compared to a reference image to calculate the displacement fields on the surface of the specimen.

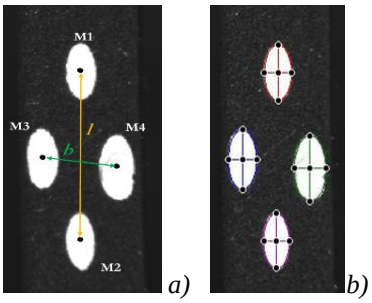

Fig. 1. Coordinates obtained employing Videotraction (a) and IAT (b)

Contrary to DIC, the IAT does not requires a searching window nor a predictive function: a bilinear polynomial function is employed to fit the displacement fields after they are measured. The fitted displacement field is then derived to calculate the deformations fields. Different formulation are implemented in the IAT: Total and Update Lagrangian, Eulerian ([8]), Logarithmic and Engineering formulations. 3D strain could be deduced under transversal isotropy hypothesis.

The IAT was validated through comparison with DIC software Correla, analyzing the images taken during a tensile test were both Videotraction markers and DIC pattern were painted on the specimen gauge length. The comparison of the deformations showed an almost perfect superposition, validating the IAT.

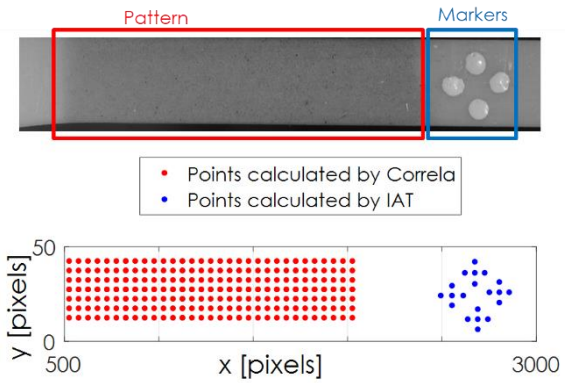

Fig. 2. Specimen employed for IAT validation: in red the pattern and in blue the markers and the coordinates of the points identified by DIC and IAT respectively

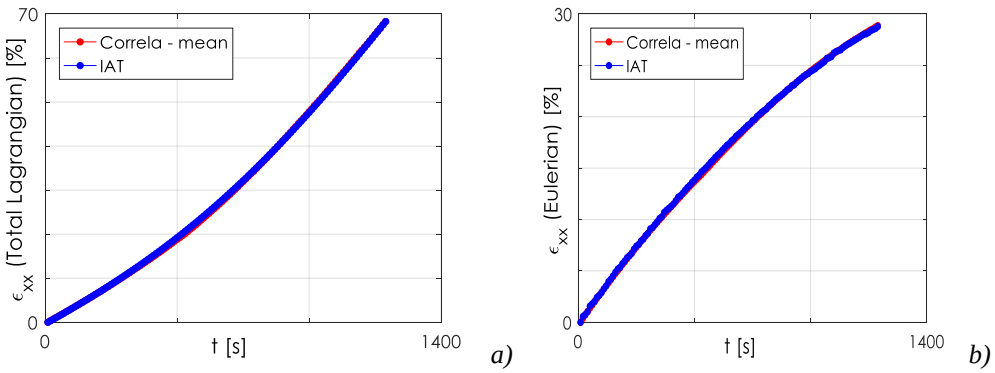

Fig. 3. Comparison between IAT and DIC results for Total Lagrangian (a) and Eulerian formulation (b)

3. Experimental tests on PEKK

In order to determine the behavior of semicrystalline PEKK at T>Tg, a mechanical characterization through tensile, DMA and creep-recovery tests, and a physical-chemical characterization, with DSC tests were carried out.

3.1 Mechanical characterization

Tensile tests were carried out at different temperatures from room temperature to 200°C, on dogbone specimens (type 1BA according to ISO 527-2), at 1 mm/min, and the results are shown in Fig. 4a: there is a decreasing of the apparent stiffness and an increasing of the ductility as the temperature increases. Furthermore, as the temperature is increased over Tg, no necking appears. The initial tensile modulus was evaluated at each temperature through a linear regression between 0.1% and 0.4% true strain.

Other tensile tests were carried out at 3 temperature above Tg (165°C, 180°C and 200°C) at different displacement speeds (0.1, 1 and 10 mm/min) to investigate time effects too. When around Tg, the increase of displacement speed produces an increase of the apparent stiffness. Instead, moving at higher temperatures, the material seems less sensitive to the temperature and time effects. Moreover, while above Tg, no pure elastic region is clearly identifiable.

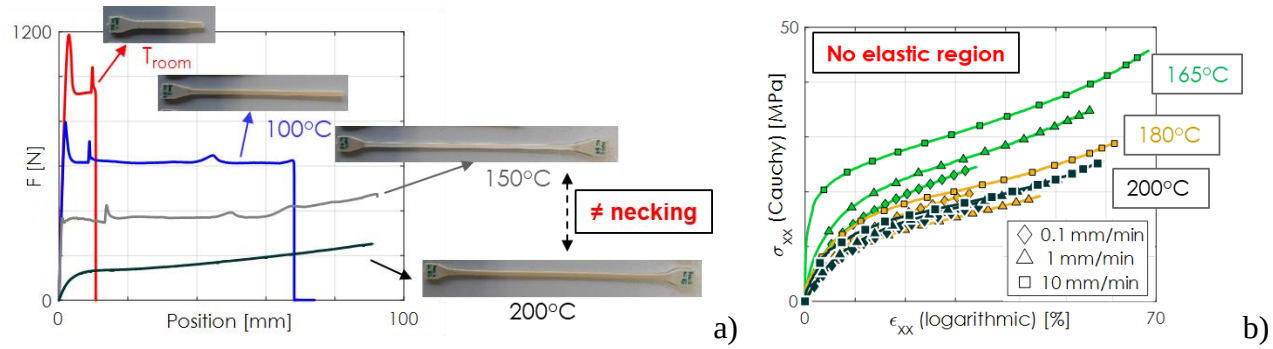

Fig. 4. Tensile test on semicrystalline PEKK from room temperature to 200°C at 1 mm/min (a) and at 165°C, 180°C and 200°C at 0.1 mm/min, 1 mm/min and 10 mm/min

3-point-bending DMA tests were carried out on 70x10x2.11 mm specimens, varying the temperature from 20°C to 200°C at 2°C/min and at 1 Hz. They show a severe decrease of the storage modulus (around 90%) as the temperature is increased over Tg. The trend of the storage modulus confirms the trend obtained evaluating the initial tensile modulus and the reduced modulus obtained from indentation tests.

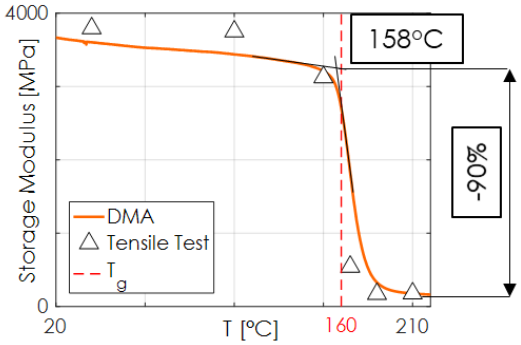

Fig. 5. DMA storage modulus between 20°C and 200°C, compared with initial tensile modulus and indentation modulus

The creep test parameters were obtained from the tensile tests: creep-recovery tests were carried out at the same 3 temperatures above Tg, with loading and unloading displacement speed of 1 mm/min at the 30%, 50% and 70% of the material threshold stresses, defined as the stress levels in correspondence of which the tangent modulus reaches the 15% of its initial value. The overall duration of test was around 1 week, divided in 48 h of creep phase and 60 h of the recovery phase. The same geometry of specimen employed for tensile tests was employed.

The deformation trend resulting from those tests is showed in Fig.6a, where an initial creep and recovery strains and a permanent strain after recovery are clearly identifiable. Analyzing those permanent strain as function of the applied creep tests and extrapolating the tendency to 0 creep stress, it appears that there is no pure viscoelastic behavior.

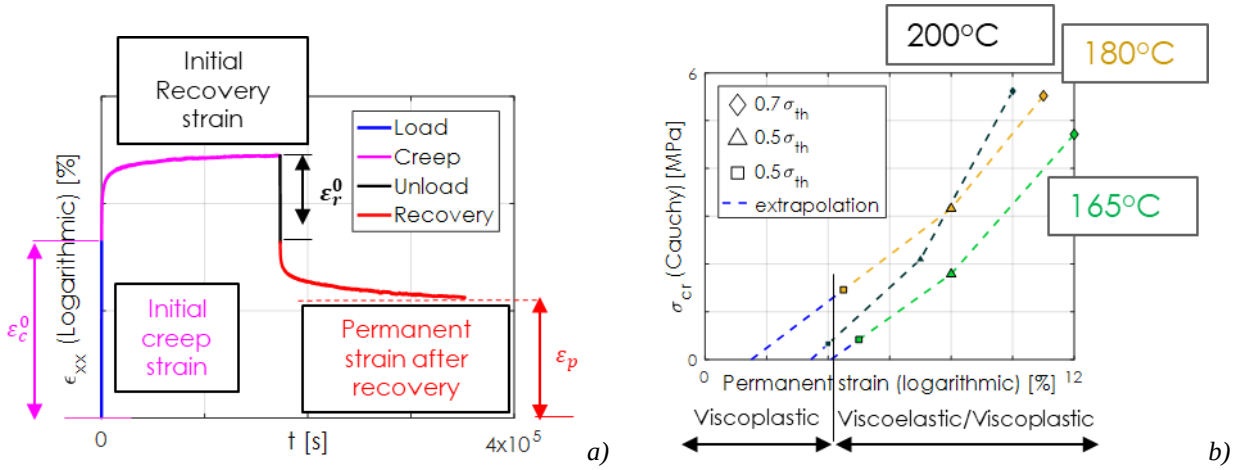

Fig. 6. DMA storage modulus between 20°C and 200°C, compared with initial tensile modulus and indentation modulus

Once evaluated the creep compliance at each testing condition, a time temperature superposition was tried, according to the Williams-Landel-Ferry (WLF) model ([9]). Since the creep tests were carried out at different stresses at different temperatures, a 2 steps procedure was employed: a first WLF law was employed to find a superposition at each temperatures, through the equation

$$Log_{10}(a_\sigma) = \frac{C_1(\sigma-\sigma_{\min})}{C_2+(\sigma-\sigma_{\min})} \qquad \text{(Eq. 1)}$$

where $\sigma_{\min}$ is the lowest creep stress applied and a_σ is the time shifting factor and then a second WLF law to superpose all the curves, through the form:

$$Log_{10}(a_t) = \frac{C_3(T-165°C)}{C_4+(T-165°C)} \qquad \text{(Eq. 2)}$$

The coefficient values are listed in Tab. 2:

T [°C]	$\sigma_{\min}$ $[MPa]$	C_1	C_2	C_3	C_4
165	5	7	9.5	10	35
180	4.5	12	14		
200	4	45	35		

Tab. 2. Coefficients of WLF law at each test temperatures

As showed in Fig. 7, it was not possible to obtain a master curve of the creep compliance, which could mean that the semicrystalline PEKK is not rheological simple, but it could have a complex behavior instead.

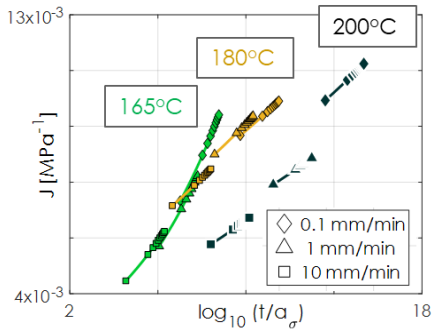

Fig. 7. WLF law applied to the creep compliance of the semicrystalline PEKK

3.2 Physical-Chemical characterization

Some samples were cut from the as-received semicrystalline PEKK and others from the previously tested specimens. Those sample were tested with DSC, varying the temperature from 20°C to 360°C, keeping the temperature constant from 5 min (preventing the material degradation), then they were cooled to 20°C and re-heated up to 360°C; all the heating and cooling ramps were carried out at 10°C/min.

The 1st heating heat flow versus temperature curves show no exothermic peak between the inflection point (corresponding to the Tg) and the endothermic peak (corresponding to the melting point): this absence implies that no cold crystallization happens, or that there is no increase in crystallinity percentage produced only by thermal loads.

Comparing the inflection points, there are negligible difference in the Tg measured values, before and after tensile and creep tests. The area of the endothermic peak gives the enthalpy of transition related to the melting of the crystalline phase and allows to evaluate the amount of crystalline percentage in the sample, trough the equation:

$$\chi = \frac{\Delta H_{melt} - \Delta H_{cold\ cryst}}{\Delta H_{100}} = \frac{Area_{peak}}{\dot{T}\ \Delta H_{100}} \qquad \text{(Eq. 1)}$$

where $\dot{T}$ is the heating rate, and ΔH_{100} =130 J/g is the theoretic endothermic enthalpy for 100% crystalline phase.

As shown in Fig. 8b, all the measured values of crystalline percentage, obtained from DSC before and after testing, are in a range of 3% of crystallinity. This leads to conclude that no morphological changes happens because of thermal-mechanical loading on semicrystalline PEKK.

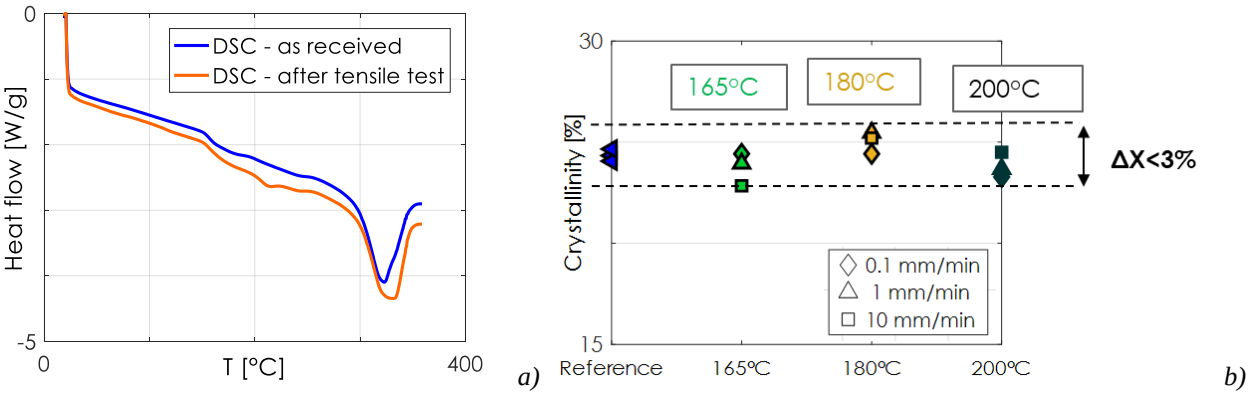

Fig. 8. Comparison between DSC heat flow vs T curves before and after tensile test (a) and comparison between crystalline percentage before and after tensile test (b)

4. Experimental tests on C/PEKK

An analogous experimental campaign was carried out on $[(\pm 45°)_2, +45°]_s$ composite specimens, to characterize the C/PEKK mechanical and physical-chemical behavior. The choice of orientation was made in such a way as to highlight the influence of the matrix.

4.1 Mechanical characterization

Tensile tests were carried out at the 3 same temperatures above Tg and 3 displacement speed applied to semicrystalline PEKK (see 3.1) and the results are showed in Fig. 9. Looking at the small deformations, there are temperature and time effects similar to the ones described for semicrystalline PEKK, suggesting not only that there could be a similarity in behavior between matrix and resin, but also that at low deformations, the composite behavior is matrix dominated. Moreover, at higher deformations, there is a more linear behavior of nominal stress as function of nominal strain, which suggests the presence of a fiber dominated region.

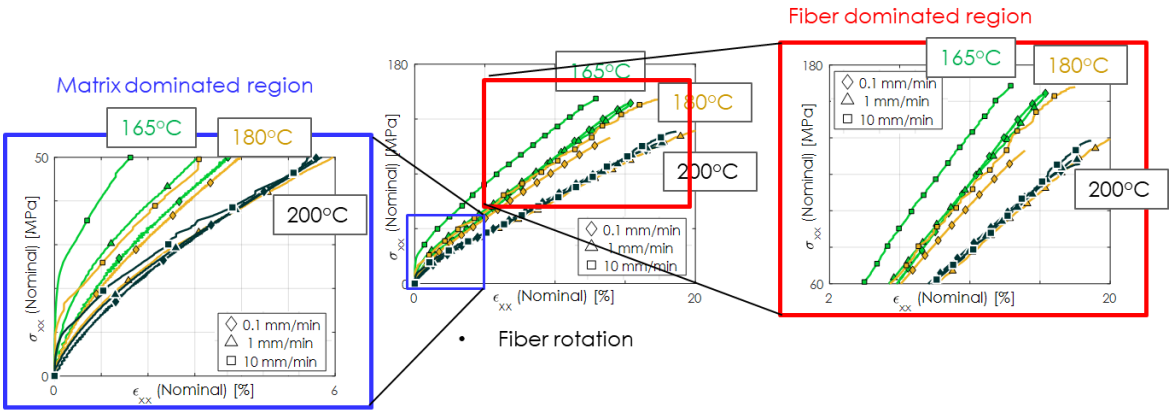

Fig. 9. Tensile test on C/PEKK composites at 165°C, 180°C and 200°C at 0.1 mm/min, 1 mm/min and 10 mm/min; on the left, matrix dominated region (low deformations) and on the right the fiber dominated region (high deformations)

The same testing protocol applied to PEKK was employed for creep-recovery tests on the composites and as parameters, the same 3 temperatures and loading and unloading displacement speed were choose. However, because of the presence of those two different regions, the creep stress were chosen differently for C/PEKK composites. For each temperature, it was defined as 1st creep stress the 50% of the composite failure stress at 1 mm/min, and as 2nd creep stress, the stress to apply to the composite which produces in the matrix an average stress field equal to the stress field applied in the resin during creep-recovery tests. An analytical method was developed to evaluate the latter stresses, which will be illustrated more in detail in Par. 4.2. The composite creep stresses are showed in Fig. 10.

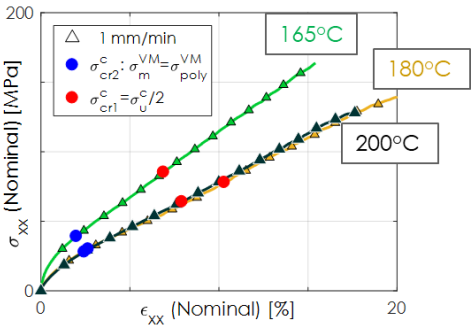

Fig. 10. Creep stress applied to the composite at 165°C, 180°C and 200°C

Looking at the results obtained from creep tests on the composite, the trend of the deformation along the tests seems similar to the one saw for the resin (Fig. 6a), still with the presence of permanent stress after the recovery.

4.2 Analytical method

The reconstruction of the composite experimental tensile test curves was carried out starting from the resin experimental data only, through a homogenization-localization method.

A first guess set of resin properties (P0) is introduced to evaluate the ply properties employing Tsai-Hill micromechanics equations ([10]). The composite properties are calculated through Herakovich's lamination theory ([11]), and, once the composite stress is introduced, it is possible to calculate the composite strain. Going downward it is also possible to calculate the ply stress and strain fields.

Freour's localization method is then employed, ([12]): this method is the adaptation of the Mori-Tanaka self-consisted method ([13]) to the case of the composite, where the ellipsoidal inclusion inside the matrix are replaced by infinite cylinders. The ply strain and properties, along the resin properties, inserted in the localization method allow to evaluate the matrix stress and strain fields.

Since both methods were developed for the linear elastic case, to describe the non-linearity of the tensile tests, matrix properties are allowed to vary according to the composite stress. At the end of the 1st step of calculation, the matrix stresses result function of the resin properties and of the composite stress ($\bar{\bar{\sigma}}_m = f\left(P_0, \bar{\bar{\sigma}}_c(j)\right)$. The matrix equivalent von Mises stress is compared to the resin equivalent von Mises stress, the latter corresponding to a specific set of resin of properties ($\sigma_m^{VM}\left(P_0, \bar{\bar{\sigma}}_c(j)\right) = \sigma_{resin}^{VM}(P_1)$. The set of properties P1 is then compared to P0 and if the difference is below a threshold, all the stress and strain fields calculated are validated, otherwise they are recalculated with the new set of resin properties P1, and the loop continues until convergence is reached. The whole procedure is then repeated for each experimental composite stress.

Fig. 11 shows the reconstruction of the tensile test curves at 1 mm/min and at 165°C, 180°C and 200°C: the model describes only the initial part of the curve, diverging rapidly at higher deformations: this seems to confirm the fact that only the initial part of the composite tensile test curve is matrix dominated and that the matrix behavior inside the composite is similar to the resin one.

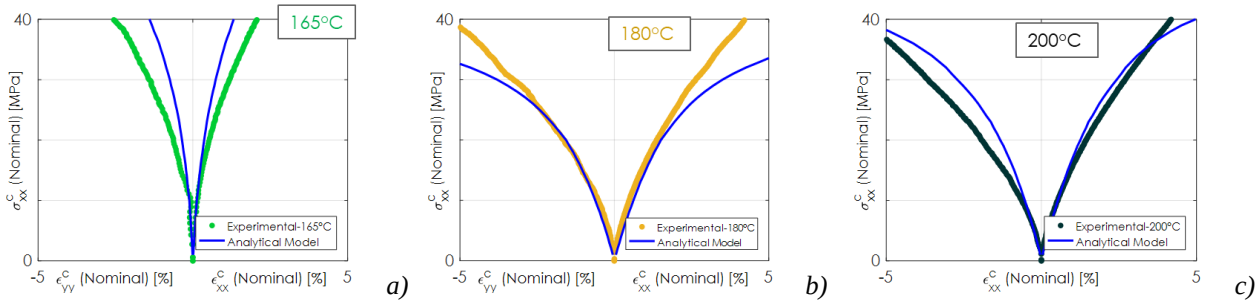

Fig. 11. Comparison between C/PEKK tensile test experimental curves and reconstructed curves with analytical model at 165°C (a), 180°C (b) and 200°C (c)

4.3 Physical-chemical characterization

DMA tests on the C/PEKK specimens were carried out with the same protocol applied to the resin and compared to the resin storage modulus vs temperature curve. The C/PEKK tensile modulus, calculated through a linear regression between 0.01% and 0.3% nominal deformation, was added to the comparison.

To simplify the comparison all the modulus were normalized respect to their initial values and the results are showed in Fig. 12. The loss of properties is anticipated in the C/PEKK and is lower (80%) compared to the PEKK, when the temperature is increased over Tg. Moreover, there is a lower agreement between the tensile moduli and the storage modulus compared to what has been seen for the resin.

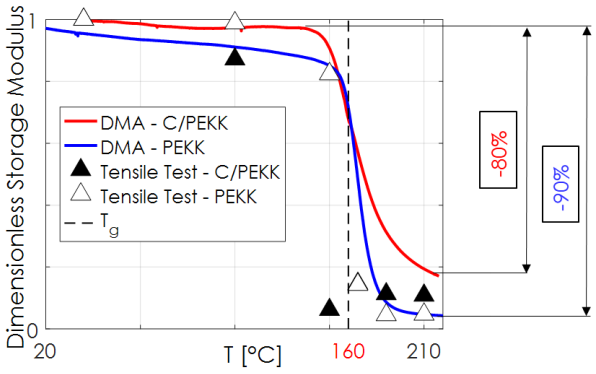

Fig. 12. Comparison between dimensionless C/PEKK DMA storage modulus between 20°C and 210°C, C/PEKK initial tensile modulus, PEKK DMA storage modulus between 20°C and 210°C and PEKK initial tensile modulus

DSC tests on the as-received C/PEKK were carried out: because of the presence of the fibers, it was not possible to precisely determine the mass of the matrix inside the samples, therefore the comparison with the DSC carried out on the PEKK, showed in Fig. 13, can only be qualitative.

The C/PEKK either shows no presence of the exothermic peak, meaning that the matrix does not increases its crystalline percentage only because of thermal load. The comparison of C/PEKK and PEKK heat flow vs temperature curves during 1st heating, shows small difference in Tg and melting peak values.

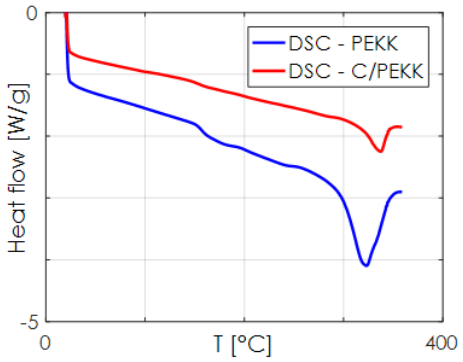

Fig. 13. Comparison between DSC heat flow vs T curves for as-received C/PEKK and PEKK

5. Conclusion and perspectives

An experimental campaign on the semicrystalline PEKK 7002 was carried out in order to describe its behavior between Tg (160°C) and 200°C. The DMA and tensile tests show that there is no significant containment of the properties loss produced by the presence of the crystalline phase when the temperature is increased over Tg. Moreover, the material becomes lesser sensitive to temperature and time effects as the temperature is increased over Tg.

The DSC tests show that there are no morphological changes in the analyzed temperature range due to thermal-mechanical loads and, combined to the absence of physical ageing and oxidation phenomena, this seems to point to the possibility of PEKK being a rheological simple material.

However, the presence of permanent deformations at the end of creep-recovery tests and the impossibility to obtain a time-temperature superposition of the creep compliances with a WLF law, denies this possibility, revealing a complex behavior instead.

A similar experimental campaign was carried out on the C/PEKK composite in order to verify if the behavior of the matrix inside the composite is similar to the resin's one. The results of both tensile and creep-recovery tests seem to confirm this similarity, at least in the low deformation region. The possibility to employ a homogenization-localization analytical method, able to describe this region only employing the resin properties, could be another confirmation. However, DMA and DSC tests show some discrepancy between the matrix and resin behaviors.

To better answer to those questions, a behavior law will be described and employed for FEM simulations on the C/PEKK.

Acknowledgement

This work pertains to the French government programs "IMPEKKABLE" (reference ANR-15-CE08-0016) and is in collaboration with AIRBUS GROUP SAS Département Innovations, ARKEMA France, Ecole Nationale Supérieure d'Arts et Métiers - Laboratoire de Procédés et Ingénierie en Mécanique et Matériaux. Thanks to Airbus Group SAS and especially to Dr. A. Vinet for the tensile tests on the C/PEKK at T<Tg. Thanks to other participants at the IMPEKKABLE project for Pprime : S. Castagnet, O. Smerdova, M.C. Lafarie. Thanks also to: F. Foti, V. Caccuri, M. Morriset, D. Mellier, J. Lefort and the whole équipe technique.

References

[1] L. Martineau, F. Chabert, G. Bernhart, T. Djilali, « Mechanical behavior of amorphous PEEK in the rubbery state. », in: ECCM17 - 17th European Conference on Composite Materials, 26 June 2016 - 30 June 2016 (Munich, Germany)
[2] L. C. Brinson, T. S. Gates, « Effects of physical aging on long term creep of polymers and polymer matrix composites », *Int. J. Solids Structures* Vol. 32 n° 6/7, pp. 827-846, 1995.
[3] Y. Guo, R. D. Bradshaw, « Isothermal physical aging characterization of Polyether-ether-ketone (PEEK) and Polyphenylene sulfide (PPS) films by creep and stress relaxation. », Mech. Time-Depend. Mater, Vol. 11, Issue 1, pp. 61-89, 2007.
[4] T. Choupin. «Mechanical performances of PEKK thermoplastic composites linked to their processing parameters. » Ph.D. thesis, ENSAM, 2017.
[5] A. Vinet, B. Fayolle, M. Gigliotti, B. Brulé, « Comportement des matrices PEKK en oxydation », in : Comptes-rendus des 21èmes Journées Nationales sur les Composites, Bordeaux INP .
[6] S. Chelaghma, O. De Almeida, P. Marguerès, J. C. Passieux, J. N. Péric, A. Vinet, B. Reine, « Investigation of PEKK crystal morphology and modelling of the crystallization kinetic of PEKK composites » in : Comptes-rendus des 20èmes Journées Nationales sur les Composites, École des Ponts ParisTech, pp. 859–868, 2017
[7] M. A. Sutton, J. J. Orteu, H. W. Schreier, «Image Correlation for Shape, Motion and Deformation Measurements. Basic Concepts, Theory and Applications », Springer, 2009.
[8] M. E. Gurtin, E. Fried, L. Anand, « The Mechanics and Thermodynamics of Continua », Cambridge University Press, 2010.
[9] M. L. Williams, R. F. Landel, J. D. Ferry, « The Temperature Dependence of Relaxation Mechanism in Amorphous Polymers and Other Glass-forming Liquids. », *J. Am. Chem. Soc.*, 77, 14, pp. 3701-3707, 1955.
[10] J. C. Halpin, S. W. Tsai, « Environmental factors in composite design », Air Force Materials Laboratory Technical Report, AFML-TR-67-423, 1967.
[11] C.T. Herakovich, « Mechanics of Fibrous Composites », John Wiley and Sons Inc., New York, 1998.
[12] S. Fréour, F. Jacquemin, R. Guillen, « On an analytical Self-Consistent model for internal stress prediction in fiber-reinforced composites submitted to hygroelastic load », *Journal of Reinforced Plastics and Composites*, 24, pp.1365-1377, 2005.
[13] T. Mori, K. Tanaka, « Average stress in matrix and average elastic energy of metals with misfitting inclusion », Acta Metallurgica, Vol. 21, pp.571-574, 1973.